

Warm Dark Matter from Theory and Galaxy Observations

H. J. de Vega

LPTHE, CNRS/Université P & M Curie (Paris VI).

**Workshop CIAS Meudon 2011: 'WARM DARK MATTER IN THE GALAXIES:
THEORETICAL AND OBSERVATIONAL PROGRESSES'**

Observatoire de Paris, Château de Meudon, Meudon campus 8, 9 and 10 June 2011

Standard Cosmological Model: DM + Λ + Baryons + Radiation

- Begins by the **inflationary** era. Slow-Roll inflation explains horizon and flatness.
- Gravity is described by Einstein's General Relativity.
- Particle Physics described by the Standard Model of Particle Physics: $SU(3) \otimes SU(2) \otimes U(1) =$ qcd+electroweak model.
- Dark matter is non-relativistic during the matter dominated era where structure formation happens. DM is outside the SM of particle physics.
- Dark energy described by the cosmological constant Λ .

Standard Cosmological Model: Λ CDM \Rightarrow Λ WDM

Dark Matter + Λ + Baryons + Radiation

begins by the Inflationary Era. **Explains** the Observations:

- Seven years WMAP data and further CMB data
- Light Elements Abundances
- Large Scale Structures (LSS) Observations. BAO.
- Acceleration of the Universe expansion:
Supernova Luminosity/Distance and Radio Galaxies.
- Gravitational Lensing Observations
- Lyman α Forest Observations
- Hubble Constant and Age of the Universe Measurements
- Properties of Clusters of Galaxies
- Galaxy structure explained by WDM

Universe Inventory

The universe is spatially flat: $ds^2 = dt^2 - a^2(t) d\vec{x}^2$
plus small primordial fluctuations.

Dark Energy (Λ): 74 % , Dark Matter: 21 %

Baryons + electrons: 4.4 % , Radiation ($\gamma + \nu$): 0.0085%

83 % of the matter in the Universe is **DARK**.

$$\rho(\text{today}) = 0.974 \cdot 10^{-29} \frac{\text{g}}{\text{cm}^3} = 5.46 \frac{\text{GeV}}{\text{m}^3} = (2.36 \cdot 10^{-3} \text{ eV})^4$$

DM dominates in the **halos** of galaxies (external part).

Baryons dominate around the **center** of galaxies.

Galaxies form out of matter collapse. Since angular momentum is conserved, when matter collapses its velocity increases. If matter can lose energy radiating, it can fall deeper than if it cannot radiate.

Kinetic Theory in Cosmology

Distribution function in phase-space: $f(t, p_i, x^i)$, $i = 1, 2, 3$

Boltzmann-Vlasov equation:

$$\frac{df}{dt} = \frac{\partial f}{\partial t} + \frac{p^i}{p^0} \frac{\partial f}{\partial x^i} + \frac{dp_i}{dt} \frac{\partial f}{\partial p_i} = \text{Collision terms}$$

Geodesic equations:

$$\frac{dx^\alpha}{dt} = \frac{p^\alpha}{p^0}, \quad \frac{dp_\alpha}{dt} = -\frac{1}{2 p^0} p_\beta p_\gamma \frac{\partial g^{\beta\gamma}}{\partial x^\alpha}, \quad 0 \leq \alpha, \beta, \gamma \leq 3$$

The **Einstein** equations determine the metric $g_{\alpha\beta}(t, x^i)$ in terms of the matter+radiation distribution function given by $f(t, p_i, x^i) \Rightarrow$ the Boltzmann-Vlasov equation becomes **non-linear**.

Collision terms **negligible** after particle decoupling.

The Boltzmann-Vlasov equation **can be linearized** around the FRW cosmological geometry before structure formation.

Dark Matter

DM particles can decouple being **ultrarelativistic** (UR) at $T_d \gg m$ or non-relativistic $T_d \ll m$.

We consider particles that decouple **at or out** of LTE (LTE = local thermal equilibrium).

Distribution function: $F_d[p_c]$ **freezes out** at decoupling.

p_c = comoving momentum.

$P_f(t) = p_c/a(t)$ = Physical momentum,

Velocity fluctuations: $Q = P_f(t)/T_d(t) = p_c/T_d$

$$\langle \vec{V}^2(t) \rangle = \left\langle \frac{\vec{P}_f^2(t)}{m^2} \right\rangle = \left[\frac{T_d}{m a(t)} \right]^2 \frac{\int_0^\infty Q^4 F_d(Q) dQ}{\int_0^\infty Q^2 F_d(Q) dQ} .$$

Energy Density: $\rho_{DM}(t) = \frac{m g}{2\pi^2} \frac{T_d^3}{a^3(t)} \int_0^\infty Q^2 F_d(Q) dQ ,$

g : # of internal degrees of freedom of the DM particle, $1 \leq g \leq 4$. Formula valid at times when DM particles are non-relativistic.

Dark Matter density and DM velocity dispersion

Using entropy conservation: $T_d = \left(\frac{2}{g_d}\right)^{\frac{1}{3}} T_{cmb}$,

g_d = effective # of UR degrees of freedom at decoupling,

$T_{cmb} = 0.2348 \cdot 10^{-3}$ eV, and

$$\frac{m}{\pi^2} \frac{g}{g_d} T_{cmb}^3 \int_0^\infty Q^2 F_d(Q) dQ = \rho_{DM}(\text{today}) = 1.107 \frac{\text{keV}}{\text{cm}^3} \quad (1)$$

We obtain for the **primordial** velocity dispersion:

$$\sigma_{prim}(z) = \sqrt{\frac{1}{3} \langle \vec{V}^2 \rangle(z)} = 0.05124 \frac{1+z}{g_d^{\frac{1}{3}}} \left[\frac{\int_0^\infty Q^4 F_d(Q) dQ}{\int_0^\infty Q^2 F_d(Q) dQ} \right]^{\frac{1}{2}} \frac{\text{keV}}{m} \frac{\text{km}}{\text{s}}$$

Goal: determine m and g_d . We need **TWO constraints**.

Notice that $F_d(Q)$ and $I_{2n} = \int_0^\infty Q^{2n} F_d(Q) dQ$, $n = 1, 2$.

are quantities **of order one**.

The Phase-space density $Q = \rho/\sigma^3$ and its decrease factor Z

The phase-space density $Q \equiv \rho/\sigma^3$ is **invariant** under the cosmological expansion and can **only decrease** under self-gravity interactions (gravitational clustering).

The phase-space density **today** follows observing dwarf spheroidal satellite galaxies of the Milky Way (dSphs)

$$\frac{\rho_s}{\sigma_s^3} \sim 5 \times 10^3 \frac{\text{keV/cm}^3}{(\text{km/s})^3} = (0.18 \text{ keV})^4 \quad \text{Gilmore et al. 07 and 08.}$$

During structure formation ($z \lesssim 30$), $Q = \rho/\sigma^3$ **decreases** by a factor that we call Z , ($Z > 1$):

$$Q_{today} = \frac{1}{Z} Q_{prim} \quad , \quad Q_{prim} = \frac{\rho_{prim}}{\sigma_{prim}^3} = \frac{3 \sqrt{3}}{2 \pi^2} g \frac{I_2^{\frac{5}{2}}}{I_4^{\frac{3}{2}}} m^4 \quad , \quad (2).$$

$$I_{2n} = \int_0^\infty Q^{2n} F_d(Q) dQ \quad , \quad n = 1, 2.$$

The spherical model gives $Z \simeq 41000$ and N -body simulations indicate: $10000 > Z > 1$. Z is **galaxy dependent**.

Mass Estimates for DM particles

Constraints: **First** $\rho_{DM}(\text{today})$, **Second** $Q_{\text{today}} = \rho_s / \sigma_s^3$

Combining the previous expressions lead to **general formulas** for m and g_d :

$$m = \frac{2^{\frac{1}{4}} \sqrt{\pi}}{3^{\frac{3}{8}} g^{\frac{1}{4}}} Z^{\frac{1}{4}} Q_{\text{today}}^{\frac{1}{4}} \frac{I_4^{\frac{3}{8}}}{I_2^{\frac{5}{8}}}, \quad g_d = \frac{2^{\frac{1}{4}} g^{\frac{3}{4}}}{3^{\frac{3}{8}} \pi^{\frac{3}{2}} \Omega_{DM}} \frac{T_\gamma^3}{\rho_c} Q_{\text{today}}^{\frac{1}{4}} Z^{\frac{1}{4}} [I_2 I_4]^{\frac{3}{8}}$$

where: $Q_{\text{today}}^{\frac{1}{4}} = 0.18 \text{ keV}$ from the dSphs data,

$$T_\gamma = 0.2348 \text{ meV}, \quad \Omega_{DM} = 0.228, \quad \rho_c = (2.36 \text{ meV})^4$$

These formulas yield for relics decoupling **UR at LTE**:

$$m = \left(\frac{Z}{g}\right)^{\frac{1}{4}} \text{ keV} \begin{cases} 0.568 \\ 0.484 \end{cases}, \quad g_d = g^{\frac{3}{4}} Z^{\frac{1}{4}} \begin{cases} 155 \text{ Fermions} \\ 180 \text{ Bosons} \end{cases}.$$

Since $g = 1 - 4$, we see that $g_d \gtrsim 100 \Rightarrow T_d \gtrsim 100 \text{ GeV}$.

$1 < Z^{\frac{1}{4}} < 10$ for $1 < Z < 10000$. **Example:** for DM Majorana fermions ($g = 2$) $0.5 \text{ keV} \lesssim m \lesssim 5 \text{ keV}$.

Out of thermal equilibrium decoupling

Results for m and g_d on the **same** scales for DM particles decoupling UR **out of thermal equilibrium**.

For the χ model of sterile neutrinos where decoupling is out of thermal equilibrium:

$$0.56 \text{ keV} \lesssim m_\nu Z^{-\frac{1}{4}} \lesssim 1.0 \text{ keV} \quad , \quad 15 \lesssim g_d Z^{-\frac{1}{4}} \lesssim 84$$

$$\text{Therefore, } 0.6 \text{ keV} \lesssim m_\nu \lesssim 10 \text{ keV} \quad , \quad 20 \lesssim g_d \lesssim 850.$$

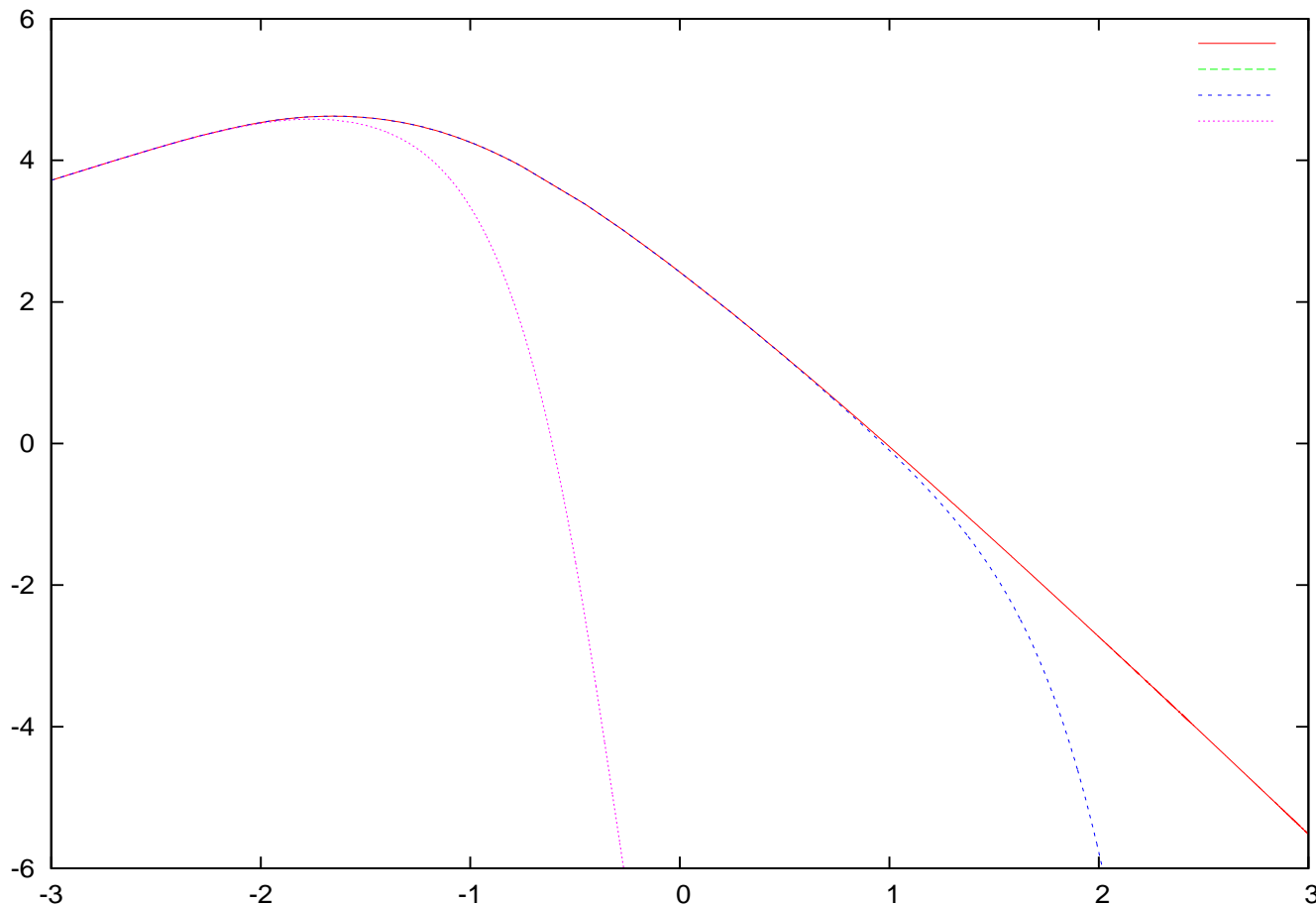
Relics decoupling non-relativistic:

similar bounds: $\text{keV} \lesssim m \lesssim \text{MeV}$

D. Boyanovsky, H. J. de Vega, N. Sanchez,
Phys. Rev. D 77, 043518 (2008), arXiv:0710.5180.

H. J. de Vega, N. G. Sanchez, MNRAS 404, 885 (2010),
arXiv:0901.0922.

Linear primordial power today $P(k)$ vs. k Mpc h

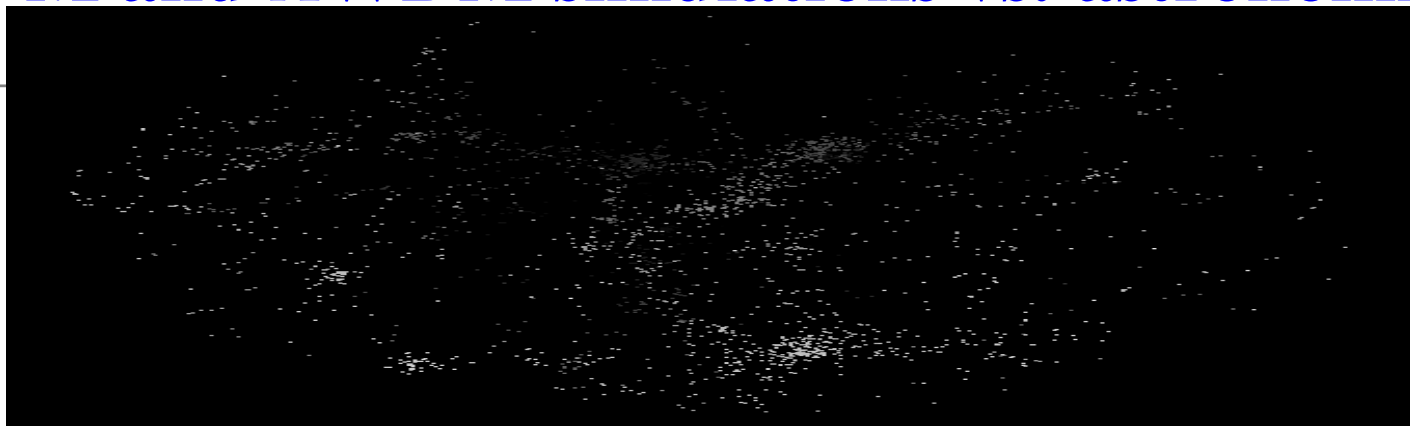


$\log_{10} P(k)$ vs. $\log_{10}[k \text{ Mpc } h]$ for **WIMPS**, **1 keV** DM particles and **10 eV** DM particles. $P(k) = P_0 k^{n_s} T^2(k)$.

$P(k)$ cutted for **1 keV** DM particles on scales $\lesssim 100$ kpc.

Transfer function in the MD era from Gilbert integral eq

Λ CDM and Λ WDM simulations vs. astronomical observations



wimps



observations



1 keV particles

Galaxies

Physical variables in galaxies:

a) **Nonuniversal** quantities: mass, size, luminosity, fraction of DM, DM core radius r_0 , central DM density ρ_0 , ...

b) **Universal** quantities: surface density $\mu_0 \equiv r_0 \rho_0$ and DM density profiles. M_{BH}/M_{halo} (or the halo binding energy).

The galaxy variables are related by **universal** empirical relations. Only **one variable** remains free.

Universal quantities may be **attractors** in the dynamical evolution.

Universal DM density profile in Galaxies:

$$\rho(r) = \rho_0 F\left(\frac{r}{r_0}\right), \quad F(0) = 1, \quad x \equiv \frac{r}{r_0}, \quad r_0 = \text{DM core radius.}$$

Empirical cored profiles: $F_{Burkert}(x) = \frac{1}{(1+x)(1+x^2)}$.

Cored profiles **do reproduce** the astronomical observations.

The constant surface density in DM and luminous galaxies

The Surface density for dark matter (DM) halos and for luminous matter galaxies defined as: $\mu_{0D} \equiv r_0 \rho_0$,

r_0 = halo core radius, ρ_0 = central density for DM galaxies

$$\mu_{0D} \simeq 120 \frac{M_{\odot}}{\text{pc}^2} = 5500 (\text{MeV})^3 = (17.6 \text{ MeV})^3$$

5 kpc < r_0 < 100 kpc. For luminous galaxies $\rho_0 = \rho(r_0)$.

Donato et al. 09, Gentile et al. 09. [$\mu_{0D} = g$ in the surface].

Universal value for μ_{0D} : **independent** of galaxy luminosity for a large number of galactic systems (spirals, dwarf irregular and spheroidals, elliptics) spanning over 14 magnitudes in luminosity and of different Hubble types.

Similar values $\mu_{0D} \simeq 80 \frac{M_{\odot}}{\text{pc}^2}$ in interstellar molecular clouds of size r_0 of different type and composition over scales $0.001 \text{ pc} < r_0 < 100 \text{ pc}$ (Larson laws, 1981).

Scaling of the energy and entropy from the surface density

Total energy using the **virial and the profile** $F(x)$:

$$\begin{aligned} E &= \frac{1}{2} \langle U \rangle = -\frac{1}{4} G \int \frac{d^3 r d^3 r'}{|r-r'|} \langle \rho(r) \rho(r') \rangle = \\ &= -\frac{1}{4} G \rho_0^2 r_0^5 \int \frac{d^3 x d^3 x'}{|x-x'|} \langle F(x) F(x') \rangle \quad \Rightarrow \quad E \sim G \mu_{0D}^2 r_0^3 \end{aligned}$$

The **energy** scales as the **volume**.

For consistency with the profile, the Boltzmann-Vlasov distribution function must scale as

$$f(\mathbf{p}, \mathbf{r}) = \frac{1}{m^4 r_0^3 G^{\frac{3}{2}} \sqrt{\rho_0}} \mathcal{F} \left(\frac{\mathbf{p}}{m r_0 \sqrt{G \rho_0}}, \frac{\mathbf{r}}{r_0} \right)$$

Hence, the entropy scales as

$$S = \int f(\mathbf{p}, \mathbf{r}) \log f(\mathbf{p}, \mathbf{r}) d^3 p d^3 r \sim r_0^3 \frac{\rho_0}{m} = r_0^2 \frac{\mu_{0D}}{m} .$$

The **entropy** scales as the **surface** (as for black-holes).

However, very different proportionality coefficients:

$$\frac{S_{BH}/A}{S_{gal}/r_0^2} \sim \frac{m}{\text{keV}} 10^{36} \Rightarrow \text{Much smaller coefficient for galaxies than for black-holes. Bekenstein bound satisfied.}$$

DM surface density from linear Boltzmann-Vlasov eq

The distribution function of the decoupled DM particles:

$f(\vec{x}, \vec{p}; t) = g f_0^{DM}(p) + F_1(\vec{x}, \vec{p}; t)$, $f_0^{DM}(p) =$ zeroth order DM distribution function in or out of thermal equilibrium.

We evolve the distribution function $F_1(\vec{x}, \vec{p}; t)$ according to the **linearized Boltzmann-Vlasov** equation since the end of inflation. The DM density fluctuations are given by

$$\Delta(t, \vec{k}) \equiv m \int \frac{d^3 p}{(2\pi)^3} \int d^3 x e^{-i \vec{x} \cdot \vec{k}} F_1(\vec{x}, \vec{p}; t)$$

Today: $\Delta(\text{today}, \vec{k}) = \rho_{DM} \bar{\Delta}(z=0, k) \sqrt{V} |\phi_k| g(\vec{k})$,

where $\bar{\Delta}(z, k)$ obeys a Volterra integral equation, the **primordial inflationary** fluctuations are:

$$|\phi_k| = \sqrt{2} \pi \frac{|\Delta_0|}{k^{\frac{3}{2}}} \left(\frac{k}{k_0} \right)^{\frac{n_s-1}{2}} , \quad g(\vec{k}) \text{ is a random gaussian field,}$$

$V =$ phase-space volume at horizon re-entering

$$|\Delta_0| \simeq 4.94 \cdot 10^{-5} , \quad n_s \simeq 0.964 , \quad k_0 = 2 \text{ Gpc}^{-1} , \quad \text{WMAP7} .$$

Linear density fluctuations today

The linearized Boltzmann-Vlasov equation can be recasted as a Volterra integral equation for the DM density fluctuations (de Vega, Sanchez, in preparation):

$$\bar{\Delta}(z, k) = h(z, k) + \frac{6}{(z+1) k r_{lin}} \int_{s_0}^s ds' \Pi\{k r_{lin}[s(z) - s']\} \bar{\Delta}(z(s'), k)$$

$$z(s) + 1 = (z_{eq} + 1) \sinh^2 s, \quad z_{eq} + 1 \simeq 3200, \quad \bar{\Delta}(\text{initial}, k) = 1$$

$h(z, k)$ = known function: contains the **memory** from previous UR evolution and the photons gravitational potential.

$$\Pi(x) \equiv \int_0^\infty Q dQ f_0^{DM}(Q) \sin(Q x),$$

$f_0^{DM}(Q)$ = zeroth order freezed-out DM distribution.

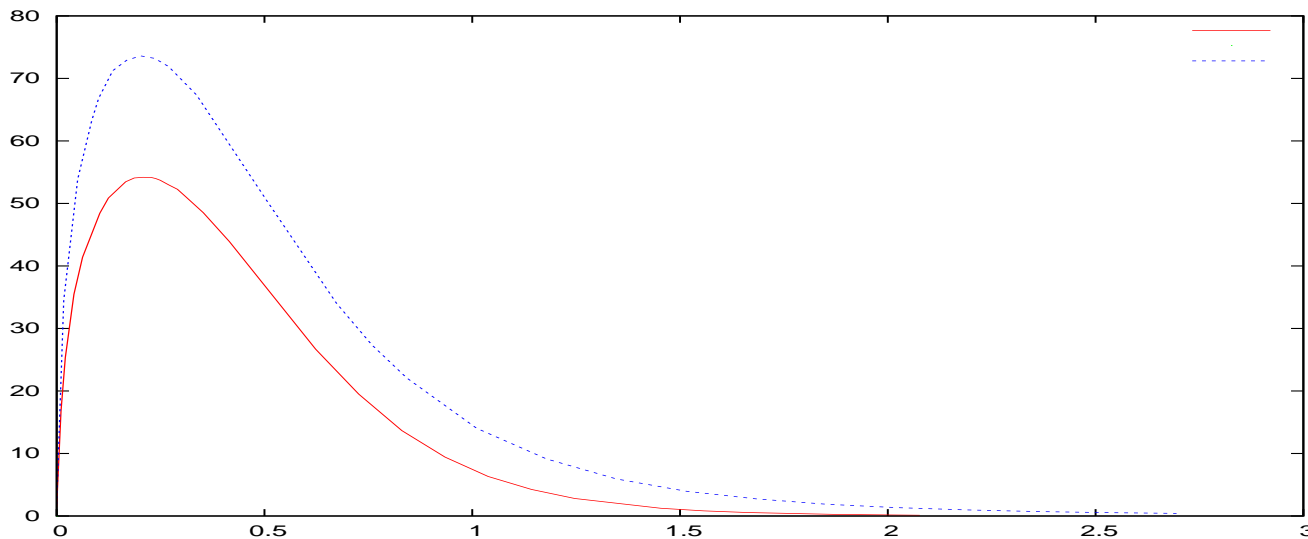
This integral equation is valid **both** in the RD and MD eras as long as the DM particles are non relativistic. It becomes the Gilbert equation in the MD era (plus memory terms).

The Free Streaming Scale

The characteristic length scale is the **free streaming scale** (or Jeans' scale)

$$r_{lin} = 2 \sqrt{1 + z_{eq}} \left(\frac{3 M_{Pl}^2}{H_0 \sqrt{\Omega_{DM}} Q_{prim}} \right)^{\frac{1}{3}} = 21.1 q_p^{\frac{1}{3}} \text{ kpc}$$

$q_p \equiv Q_{prim}/(\text{keV})^4$. DM particles can **freely** propagate over distances of the order of the free streaming scale.



Transfer function $\bar{\Delta}(z=0, k)/\bar{\Delta}(\text{initial}, k)$ vs. $k r_{lin}$. **Red**= thermal FD initial. **Blue** = χ -sterile neutrinos.

Linear density profile today

The matter density fluctuations $\rho_{lin}(r)$ are given today by

$$\rho_{lin}(r) = \frac{1}{2\pi^2 r} \int_0^\infty k dk \sin(kr) \Delta(k, t_{\text{today}}) \quad \text{for } g(\vec{k}) = 1$$

The **linear profile today** results:

$$\rho_{lin}(x) = 14.47 \rho_{DM} \frac{q_p^{\frac{n_s+2}{3}}}{x} \frac{I_3}{[(z_i+1)(z_i+1+z_{eq})]^{\frac{3}{4}}} \times \\ \times \int_0^\infty \gamma^{n_s/2-1} d\gamma \sin(\gamma x) \bar{\Delta}(z=0, \gamma)$$

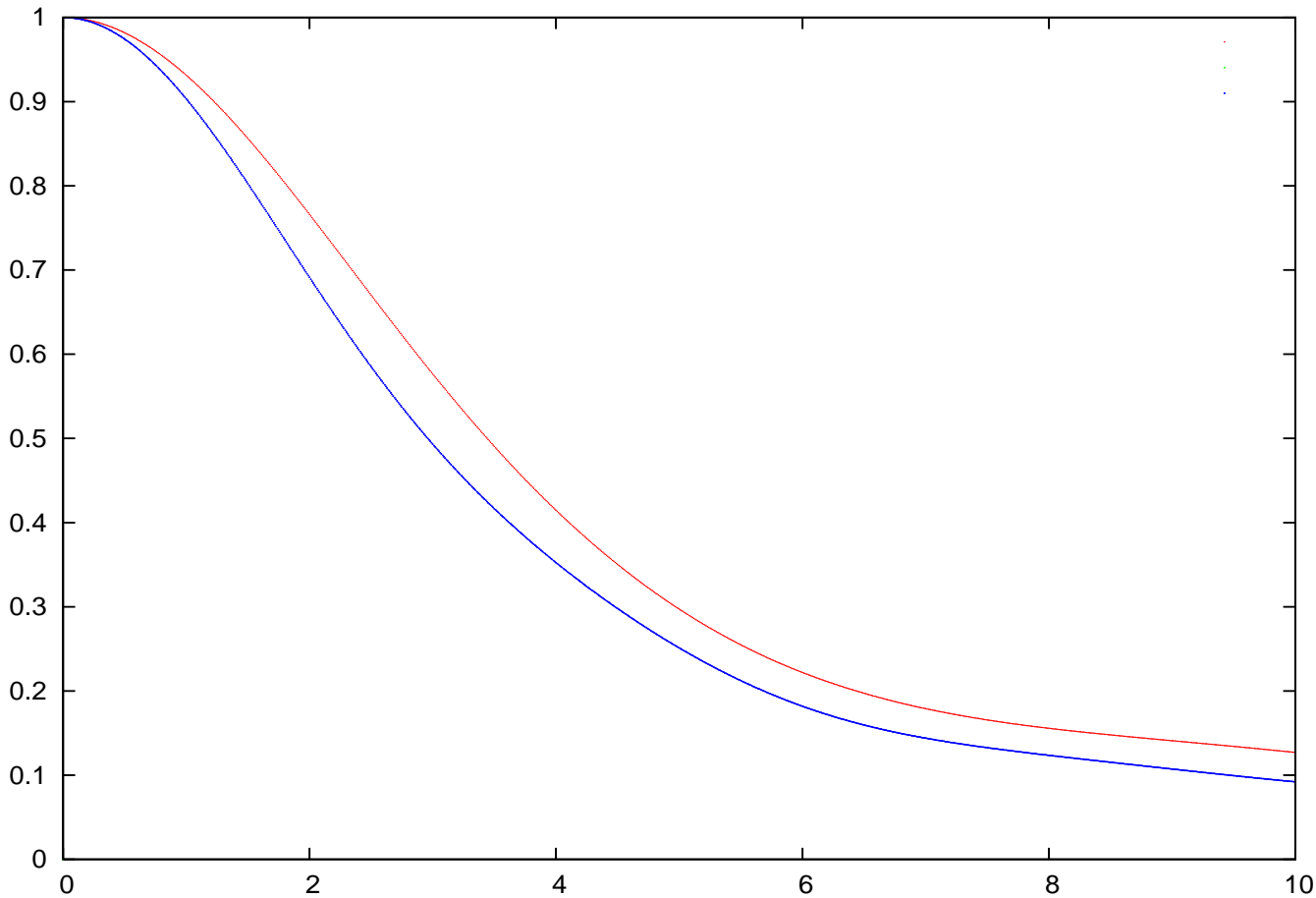
where $\gamma \equiv k r_{lin}$ and $x \equiv r/r_{lin}$.

I_n and $\bar{\Delta}(z=0, \gamma)$ depend on the freeze-out DM distribution $f_0^{DM}(Q)$.

Phase-space volume at horizon re-entering by redshift

$$z_i : V = \frac{4}{3} \pi \left(\frac{2\pi}{k_i} \right)^3, \quad k_i = H_0 \sqrt{\Omega_m (z_i + 1) \left(1 + \frac{z_i + 1}{z_{eq} + 1} \right)}$$

Density profiles in the linear approximation



Profiles $\rho_{lin}(r)/\rho_{lin}(0)$ vs. $x \equiv r/r_{lin}$.

Fermions decoupling ultrarelativistically **in** and **out** of thermal equilibrium. The halo radius r_0 is proportional to

r_{lin} : $r_0 = \beta r_{lin}$. $\beta_{in\,equil} = 5.565$, $\beta_{out\,equil} = 5.013$.

Matching the observed and the theoretical surface density

Theoretical results:

$$m/\text{keV} = q_p^{\frac{1}{4}} \begin{cases} 2.646 & \text{Thermal Fermi – Dirac,} \\ 3.144 < 2.418 \tau^{-\frac{1}{4}} < 5.591 & \chi - \text{sterile } \nu, \end{cases}$$

[0.035 < τ < 0.35: coupling in the χ sterile neutrino model.]

$$m/\text{keV} = q_p^{\frac{1}{3}} 10.447, \quad \text{DW model sterile } \nu.$$

Surface density: $\mu_0 \equiv r_0 \rho(0)$ where $r_0 =$ core radius.

$$\frac{\mu_0 \text{lin}}{(\text{MeV})^3} = \left(\frac{m}{\text{keV}} \right)^{\frac{2}{3} n_s} \frac{\mathcal{N}}{N^{\frac{3}{4}}(z_i)} \times \begin{cases} 0.2393 & \text{Thermal FD} \\ 0.2535 \tau^{n_s/6} & \chi - \text{sterile } \nu, \end{cases}$$

$$\mathcal{N} = \beta I_3 \int_0^\infty \gamma^{n_s/2} d\gamma \bar{\Delta}(\text{today}, \gamma) = \begin{cases} 348.4 & \text{Thermal FD} \\ 383.7 & \chi - \text{sterile } \nu, \end{cases}$$

$n_s = 0.964$ primordial spectral index,

$$N(z_i) \equiv (z_i + 1)(z_i + 1 + z_{eq}).$$

The DM particle mass m from the observed surface density

Matching the **observed values** $\mu_{0\text{ obs}}$ with this $\mu_{0\text{ lin}}$ gives q_p , the mass of the DM particle and g_d .

From spiral galaxies data: $\mu_{0\text{ obs}} = 6000 \text{ (MeV)}^3$ and the **DM particle mass** results,

$$\frac{m}{\text{keV}} = \left[\frac{N(z_i)}{N(100)} \right]^{\frac{9}{8n_s}} \times \begin{cases} 5.382 \text{ Fermi} - \text{Dirac} \\ 3.07 < 2.36 \tau^{-\frac{1}{4}} < 5.46 \chi - \text{sterile } \nu, \end{cases}$$

$$\frac{m}{\text{keV}} = 10.8 \left[\frac{N(z_i)}{N(100)} \right]^{\frac{3}{2n_s}}, \quad \text{DW model sterile } \nu.$$

$$N(z_i) \equiv (z_i + 1)(z_i + 1 + z_{eq})$$

UR degrees of freedom (\Rightarrow temperature) at decoupling

$$g_d = \left[\frac{N(100)}{N(z_i)} \right]^{\frac{3}{2n_s}} \times \begin{cases} 3293 \text{ Fermi} - \text{Dirac}, \\ 91 < 1124 \tau^{\frac{3}{4}} < 512 \chi - \text{sterile } \nu, \end{cases}$$

$$g_d = 22.2 \text{ DW model sterile } \nu.$$

Density profiles in the linear approximation

Density profiles turn to be **cored** at scales $r \ll r_{lin}$.

Intermediate regime $r \gtrsim r_{lin}$:

$$\rho_{lin}(r) \stackrel{r \gtrsim r_{lin}}{=} c_0 \left(\frac{r_{lin}}{r}\right)^{1+n_s/2} \rho_{lin}(0) \quad , \quad 1 + n_s/2 = 1.482.$$

$\rho_{lin}(r)$ **scales** with the **primordial spectral index** n_s .

The theoretical linear results **agree** with the universal empirical behaviour $r^{-1.6 \pm 0.4}$: M. G. Walker et al. (2009) (observations), I. M. Vass et al. (2009) (simulations).

The agreement between the linear theory and the observations is **remarkable**.

In the asymptotic regime $r \gg r_{lin}$ the small k behaviour of $\Delta(k, t_{today}) \stackrel{k \rightarrow 0}{=} c_1 (k r_{lin})^s$ with $s \simeq 0.5$ implies the presence of a tail: $\rho_{lin}(r) \stackrel{r \gg r_{lin}}{\simeq} c \left(\frac{r_{lin}}{r}\right)^2$.

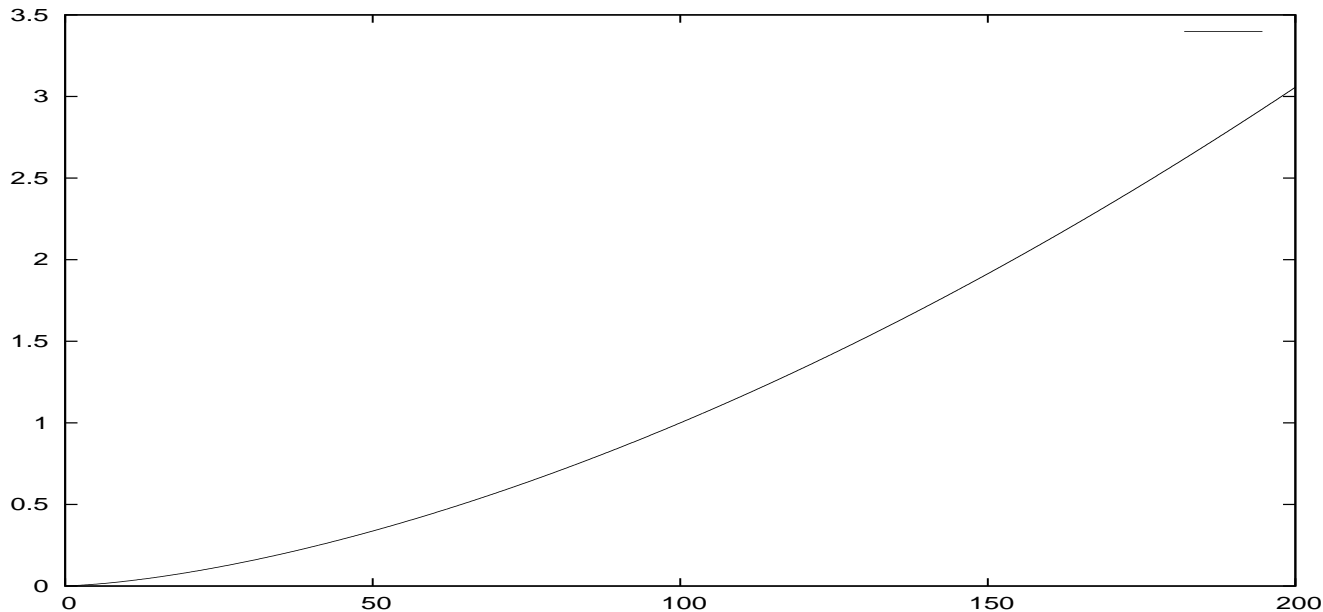
Non-universal galaxy properties.

	Observed Values
r_0	5 to 52 kpc
ρ_0	1.57 to $19.3 \times 10^{-25} \frac{\text{g}}{\text{cm}^3}$
$\sqrt{v^2_{halo}}$	79.3 to 261 km/sec

	Thermal FD	χ -sterile	DW sterile
$\frac{r_0}{\text{kpc}} \left[\frac{N(z_i)}{N(100)} \right]^{\frac{3}{2n_s}}$	36.3	86.9	36.1
$\frac{\rho_0}{10^{-25} \text{g/cm}^3} \left[\frac{N(100)}{N(z_i)} \right]^{\frac{3}{2n_s}}$	8.32	3.48	8.37
$\frac{\sqrt{v^2_{halo}}}{\text{km/sec}} \left[\frac{N(z_i)}{N(100)} \right]^{\frac{3}{4n_s}}$	218	337	217

r_0 and $\sqrt{v^2_{halo}}$ **decrease** for increasing initial redshift z_i while ρ_0 **increases** with z_i . DM particle mass: $3 < m < 11$ keV.

The dependence on the redshift z_i



The factor $[N(z_i)/N(100)]^{\frac{3}{2n_s}}$ vs. z_i .

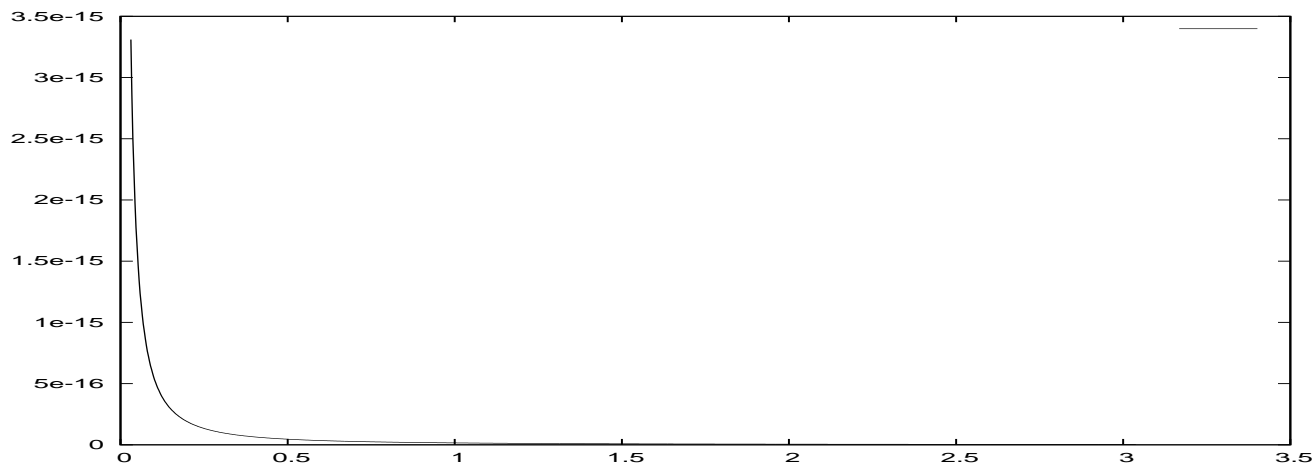
Further work:

- Effects of the random initial field $g(\vec{k})$
- Cluster of galaxies where observations indicate a surface density about eight times larger than in galaxies (Salucci et al. in preparation). This factor eight can be explained theoretically by $z_i^{galaxies} \simeq 16 z_i^{clusters}$.

Wimps vs. galaxy observations

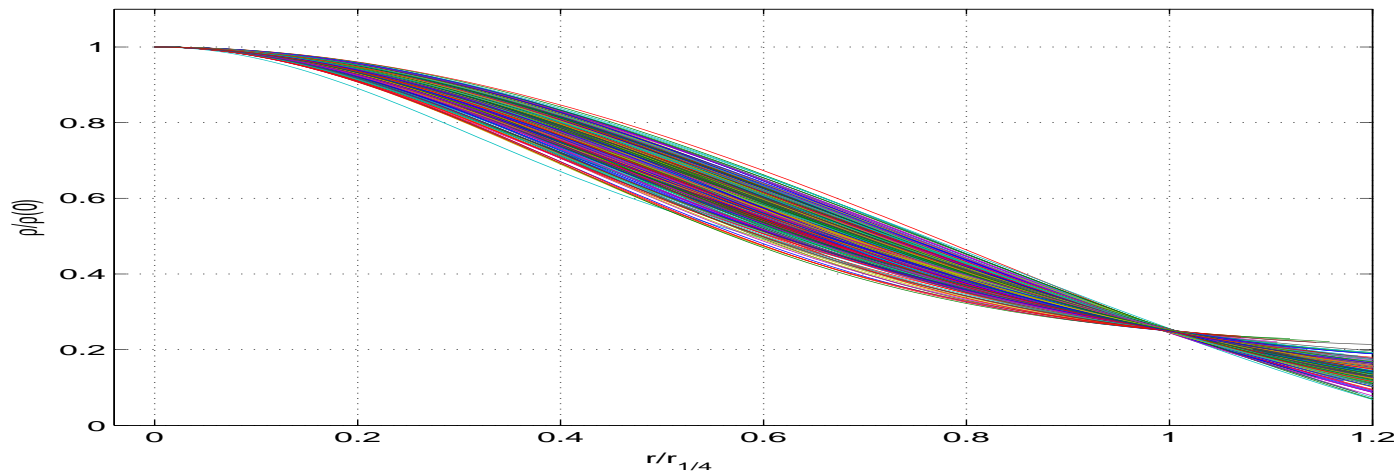
	Observed Values	Wimps in linear theory
r_0	5 to 52 kpc	0.045 pc
ρ_0	$1.57 \text{ to } 19.3 \times 10^{-25} \frac{\text{g}}{\text{cm}^3}$	$0.73 \times 10^{-14} \frac{\text{g}}{\text{cm}^3}$
$\sqrt{v^2}_{halo}$	79.3 to 261 km/sec	0.243 km/sec

The wimps values strongly disagree by **several order of magnitude** with the observations. (Here $m_{wimp} = 100 \text{ GeV}$).

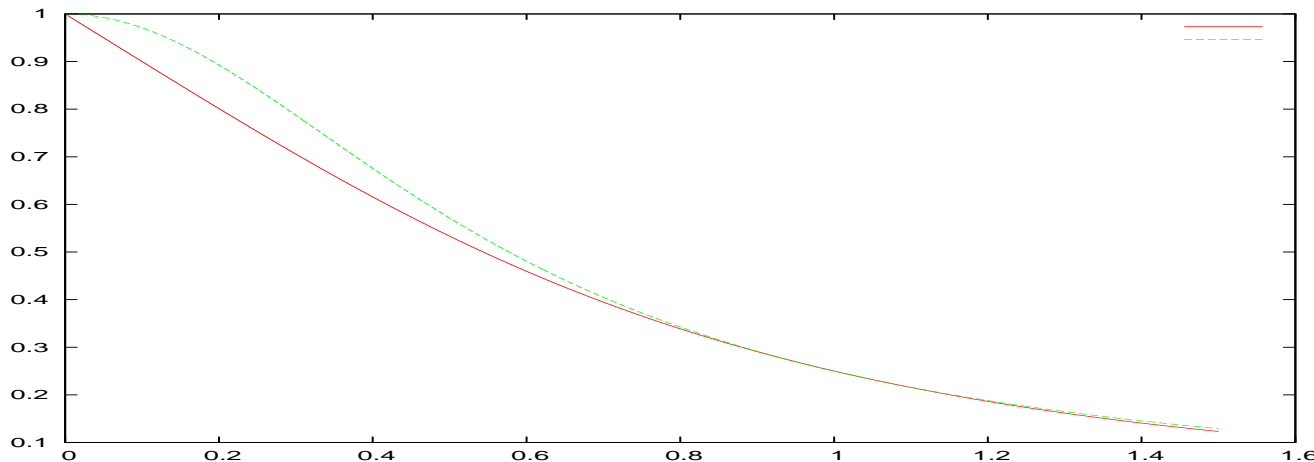


$\rho_{lin}(r)_{wimp}$ in g/cm^3 vs. r in pc. Exhibits a cusp behaviour for $r \gtrsim 0.03 \text{ pc}$.

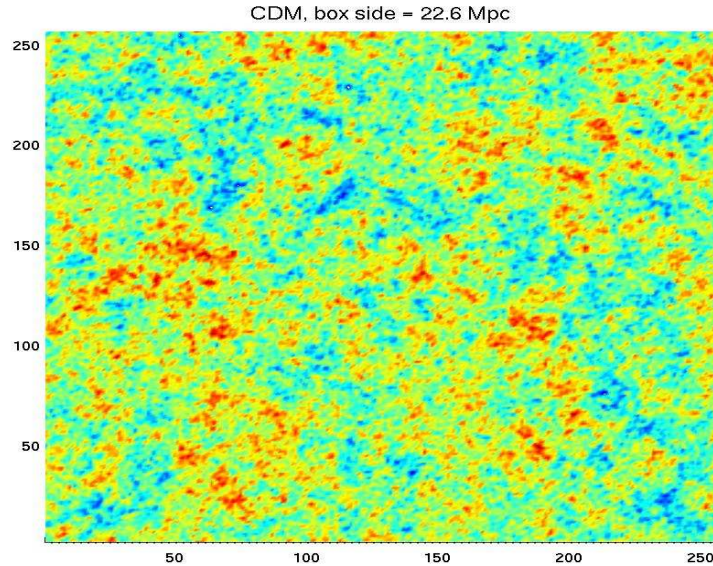
Linear evolution from random initial conditions



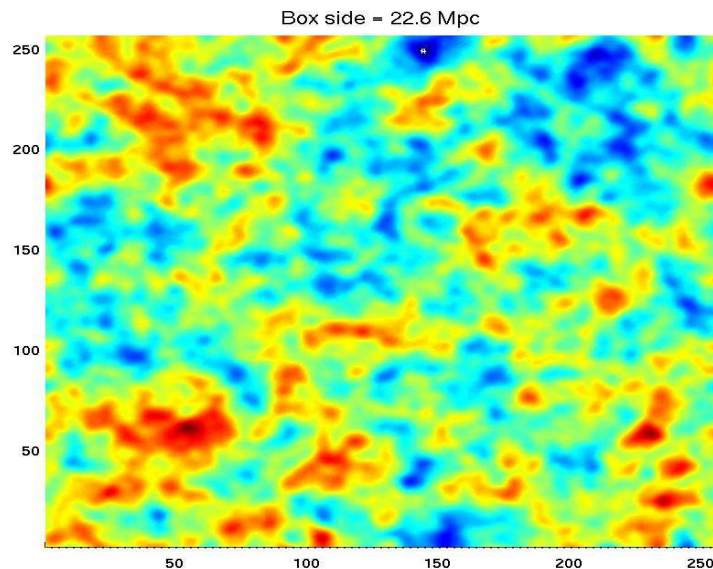
Profiles averaged in the angles for 500 random initial conditions. $\rho(r)/\rho(0)$ vs. $r/r_{1/4}$ [Destri, de Vega, Sanchez, in preparation]. **Burkert** and **Pseudothermal** profiles $\rho(r)/\rho(0)$ vs. $r/r_{1/4}$.



WDM vs. CDM linear fluctuations today



Box side = 22.6 Mpc. [Destri, de Vega, Sanchez, in preparation]



Particle physics candidates for DM

No particle in the Standard Model of particle physics (SM) can play the role of DM.

Many extensions of the SM can be envisaged to include a DM particle with mass in the **keV scale** and weakly enough coupled to the Standard Model particles to fulfill **all** particle physics experimental constraints.

Main candidates in the **keV mass scale**: **sterile neutrinos**, gravitinos, light neutralino, majoron ...

Particle physics **motivations** for sterile neutrinos:

There are both **left** and **right** handed quarks (with respect to the chirality).

It is natural to have right handed neutrinos ν_R besides the known left-handed neutrino. **Quark-lepton similarity**.

Sterile Neutrinos in the SM of particle physics

SM symmetry group: $SU(3)_{color} \otimes SU(2)_{weak} \otimes U(1)_{hypercharge}^{weak}$

Leptons are color singlets and **doublets** under weak SU(2).

Sterile neutrinos ν_R do not participate to weak interactions.

Hence, they must be **singlets** of color, weak SU(2) and weak hypercharge.

The SM Higgs Φ is a SU(2) doublet with a **nonzero** vacuum expectation value Φ_0 . It can couple Yukawa-type with the left and right handed leptons:

$$L_{Yuk} = y \bar{\nu}_L \nu_R \Phi_0 + h.c. \quad ,$$

$$y = \text{Yukawa coupling}, \quad \Phi_0 = \begin{pmatrix} 0 \\ v \end{pmatrix} \quad , \quad v = 174 \text{ GeV.}$$

This induces a mixing (bilinear) term between ν_L and ν_R which produces **transmutations** of $\nu_L \Leftrightarrow \nu_R$.

Sterile Neutrinos Mixing

Mixing and oscillations of particle states are typical of low energy particle physics !

- Flavor mixing: e- μ neutrino oscillations (explain solar neutrinos).
- $K^0 - \bar{K}^0$, $B^0 - \bar{B}^0$ and $D^0 - \bar{D}^0$ meson oscillations in connection with CP-violation.

Neutrino mass matrix: $(\bar{\nu}_L \ \bar{\nu}_R) \begin{pmatrix} 0 & m_D \\ m_D & M \end{pmatrix} \begin{pmatrix} \nu_L \\ \nu_R \end{pmatrix}$

$M =$ right-neutrino mass, $m_D = y v$, $M \gg m_D$. Seesaw.

Mass eigenvalues: $\frac{m_D^2}{M}$ and M , with eigenvectors:

- active neutrino: $\nu_{active} \simeq \nu_L - \frac{m_D}{M} \nu_R$.
- sterile neutrino: $\nu_{sterile} \simeq \nu_R + \frac{m_D}{M} \nu_L$, $M \gg m_D^2/M$.

Sterile Neutrinos

Choosing $M \sim 1$ keV and $m_D \sim 0.1$ eV is **consistent** with observations.

Mixing angle: $\theta \sim \frac{m_D}{M} \sim 10^{-4}$ is appropriate **to produce enough** sterile neutrinos accounting for the observed DM.

Smallness of θ makes sterile neutrinos difficult to detect.

Precise measure of nucleus recoil in tritium beta decay:
 ${}^3H_1 \implies {}^3He_2 + e^- + \bar{\nu}$ can show the presence of a sterile **instead** of the active $\bar{\nu}$ in the decay products.

Rhenium 187 beta decay gives $\theta < 0.095$ for 1 keV steriles [Galeazzi et al. PRL, 86, 1978 (2001)].

Available energy: $Q({}^{187}Re) = 2.47$ keV, $Q({}^3H_1) = 18.6$ keV.

Conclusion: the **empty slot** of right-handed neutrinos in the Standard Model of particle physics can be filled by **keV-scale sterile neutrinos** describing the DM.

Sterile neutrino models

Sterile neutrinos: name coined by Bruno Pontecorvo (1968).

- DW: Dodelson-Widrow model (1994) sterile neutrinos produced by non-resonant mixing from active neutrinos.
- Shi-Fuller model (1998) sterile neutrinos produced by resonant mixing from active neutrinos.
- χ -model (1981)-(2006) sterile neutrinos produced by a Yukawa coupling from a real scalar χ .
- Further models can be proposed...They must reproduce the DM cosmological density, galaxy formation and structures and be consistent with all particle physics experiments.

Summary: keV scale DM particles

- **Reproduce** the phase-space density observed in dwarf satellite galaxies and spiral galaxies (dV S 2009).
- Provide **cored** universal galaxy profiles in agreement with observations (dV S 2009, dV S S 2010).
(Review on cores vs. cusps by de Blok 2010, Salucci & Frigerio Martins 2009)
- Reproduce the universal **surface density** μ_0 of DM dominated galaxies (dV S S 2010). WIMPS simulations give 1000 times the observed value of μ_0 (Hoffman et al. 2007).
- **Alleviate** the satellite problem which appears when wimps are used (Avila-Reese et al. 2000, Götz & Sommer-Larsen 2002)
- **Alleviate** the voids problem which appears when wimps are used (Tikhonov et al. 2009).

Summary: keV scale DM particles

- All direct searches of DM particles look for $m \gtrsim 1$ GeV. DM mass in the keV scale explains why nothing has been found ... e^+ and \bar{p} excess in cosmic rays may be explained by astrophysics: P. L. Biermann et al. (2009), P. Blasi, P. D. Serpico (2009).
- Galaxies from Wimps simulations are too small (Ryan Joung et al. 2009, Holz & Perlmutter 2010). keV scale DM may alleviate this problem.
- Velocity widths in galaxies from 21cm HI surveys. ALFALFA survey clearly favours WDM over CDM. Papastergis et al. 2011, Zavala et al. 2009

Reliable simulations with keV mass DM are needed to clarify all these issues.

Summary and Conclusions

- Combining **theoretical** evolution of fluctuations through the Boltzmann-Vlasov equation with **galaxy data** points to a DM particle mass 3 - 10 keV. T_d turns to be model dependent. The keV mass scale holds **independently** of the DM particle physics model.
- Universal Surface density in DM galaxies [$\mu_{0D} \simeq (18 \text{ MeV})^3$] explained by keV mass scale DM. Density profile scales and decreases for intermediate scales with the **spectral index** n_s : $\rho(r) \sim r^{-1-n_s/2}$ and $\rho(r) \sim r^{-2}$ for $r \gg r_0$.

H. J. de Vega, P. Salucci, N. G. Sanchez, 'The mass of the dark matter particle from theory and observations', arXiv:1004.1908.

H. J. de Vega, N. Sanchez, 'Model independent analysis of dark matter points to a particle mass at the keV scale', arXiv:0901.0922, MNRAS 404, 885 (2010).

Future Perspectives

The **Golden Age** of Cosmology and Astrophysics continues.

Galaxy and Star formation. DM properties from **galaxy observations**. Early star formation. **Gigantic** AGN black-holes and their correlation with galaxy evolution.

Chandra, Suzaku X-ray data: keV mass DM decay? The **Dark** Ages...Reionisation...the 21cm line...

Sun models well reproduce the sun's chemical composition but not the **heliosismology** (Asplund et al. 2009).

Can DM inside the Sun help to explain the discrepancy?

Nature of **Dark** Matter? 83% of the matter in the universe.

Light DM particles are **strongly** favoured $m_{DM} \sim \text{keV}$.

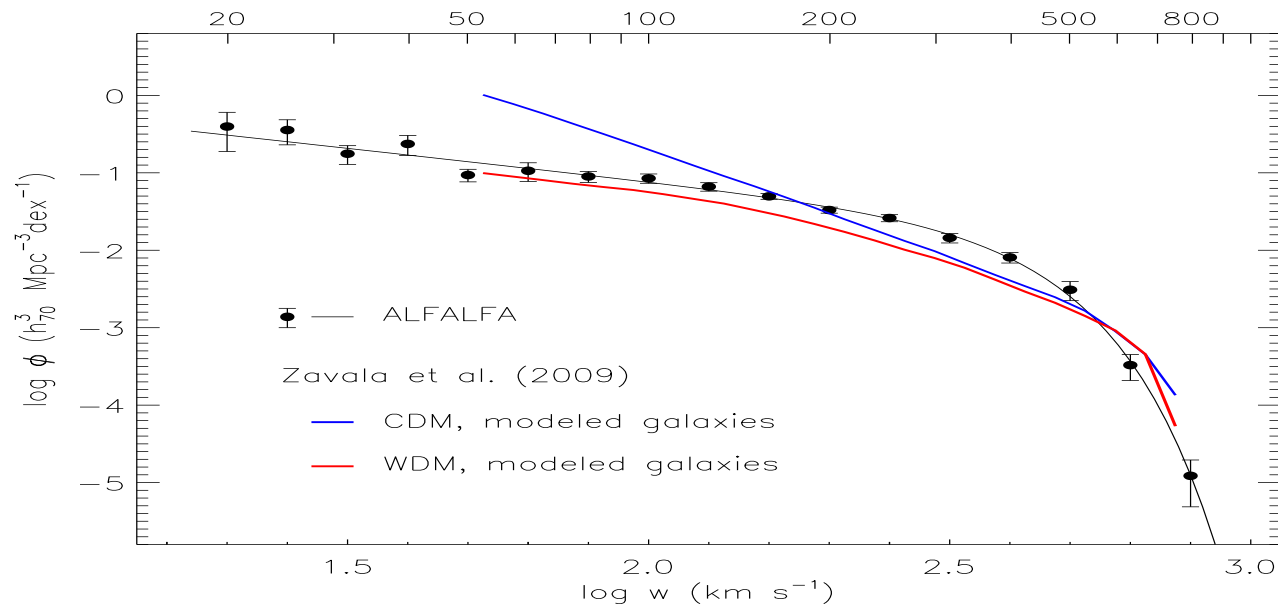
Sterile neutrinos ? Other particle in the keV mass scale?

Precision determination of DM properties (mass, T_d , nature) from **better** galaxy data combined with **theory** (Boltzmann-Vlasov and simulations).

The Universe is our ultimate physics laboratory

THANK YOU VERY MUCH
FOR YOUR ATTENTION!!

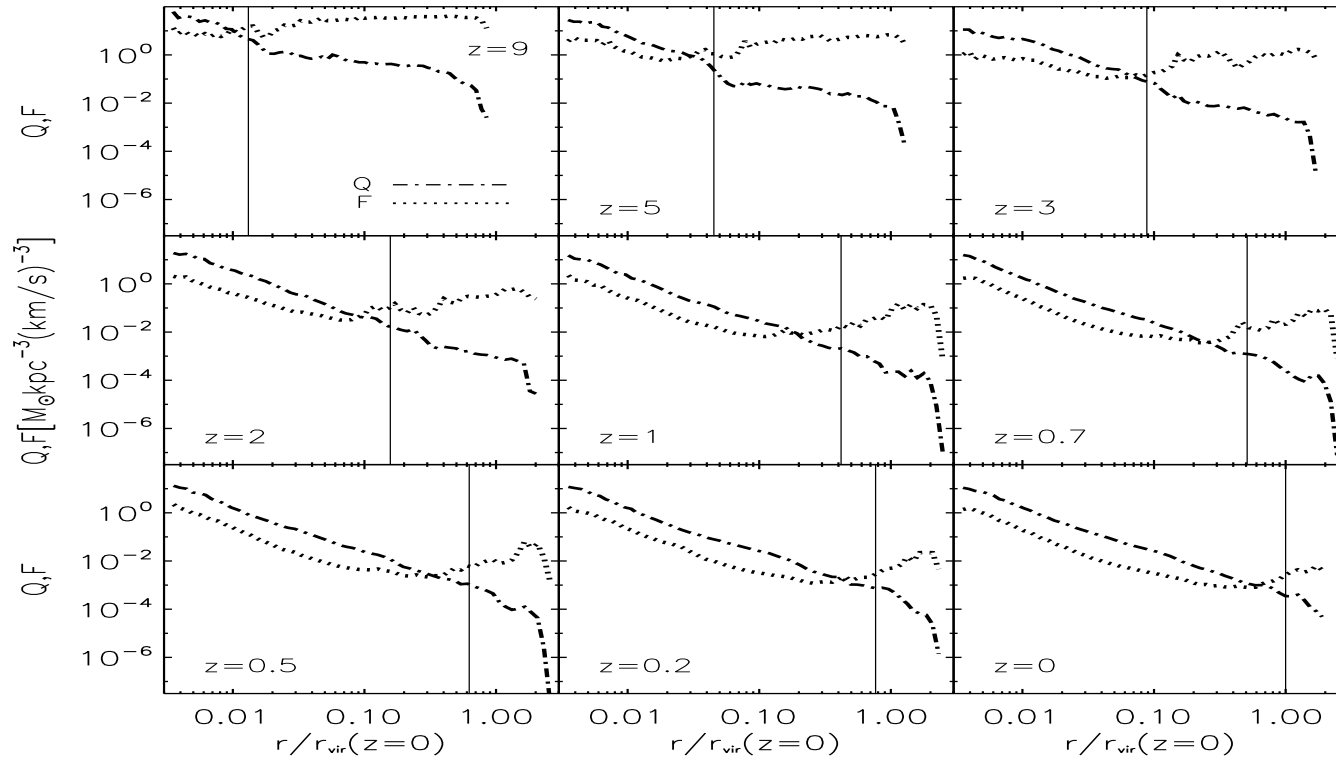
Velocity widths in galaxies



Velocity widths in galaxies from 21cm HI surveys. ALFALFA survey **clearly favours WDM** over CDM. (Papastergis et al. 2011, Zavala et al. 2009).

Notice that the WDM **red** curve is for $m = 1 \text{ keV}$.

ρ/σ^3 vs. r for different z from Λ CDM simulations

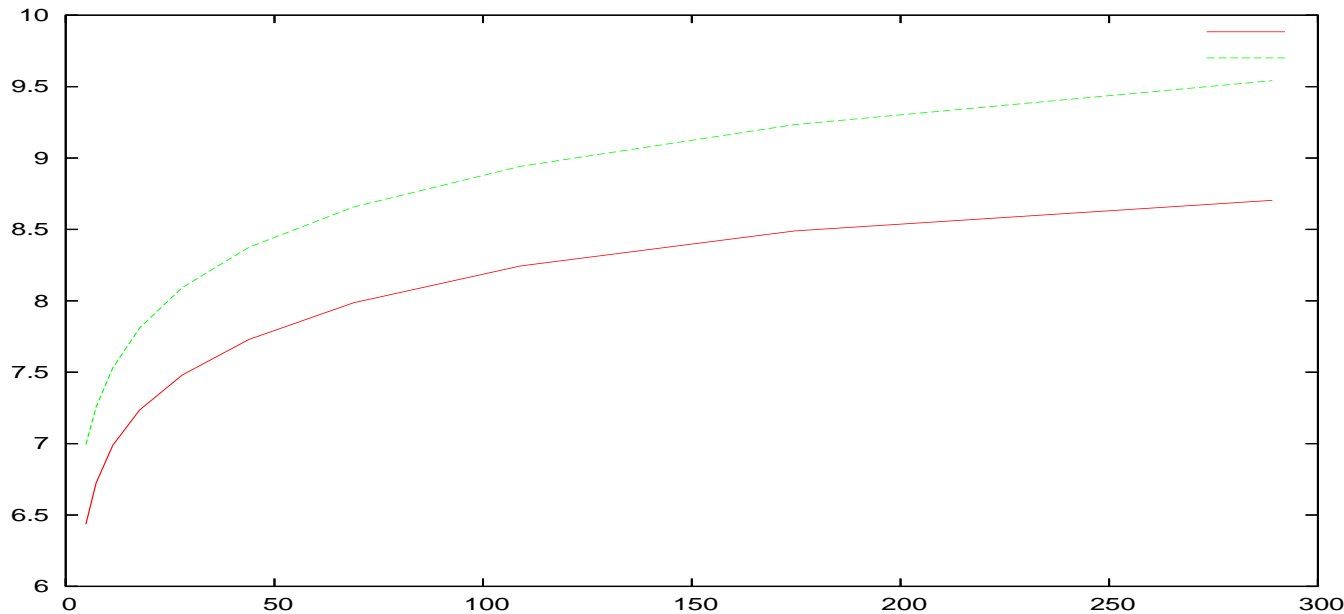


Phase-space density $Q \equiv \rho/\sigma^3$ vs. $r/r_{vir}(z=0)$ **dot-dashed line** for different redshifts: $0 \leq z \leq 9$.

We see that from $z = 9$ to $z = 0$ the r -average of ρ/σ^3 decreases by a factor $Z \sim 10$.

I. M. Vass et al. MNRAS, 395, 1225 (2009).

The self-gravity decreasing factor Z for spirals.

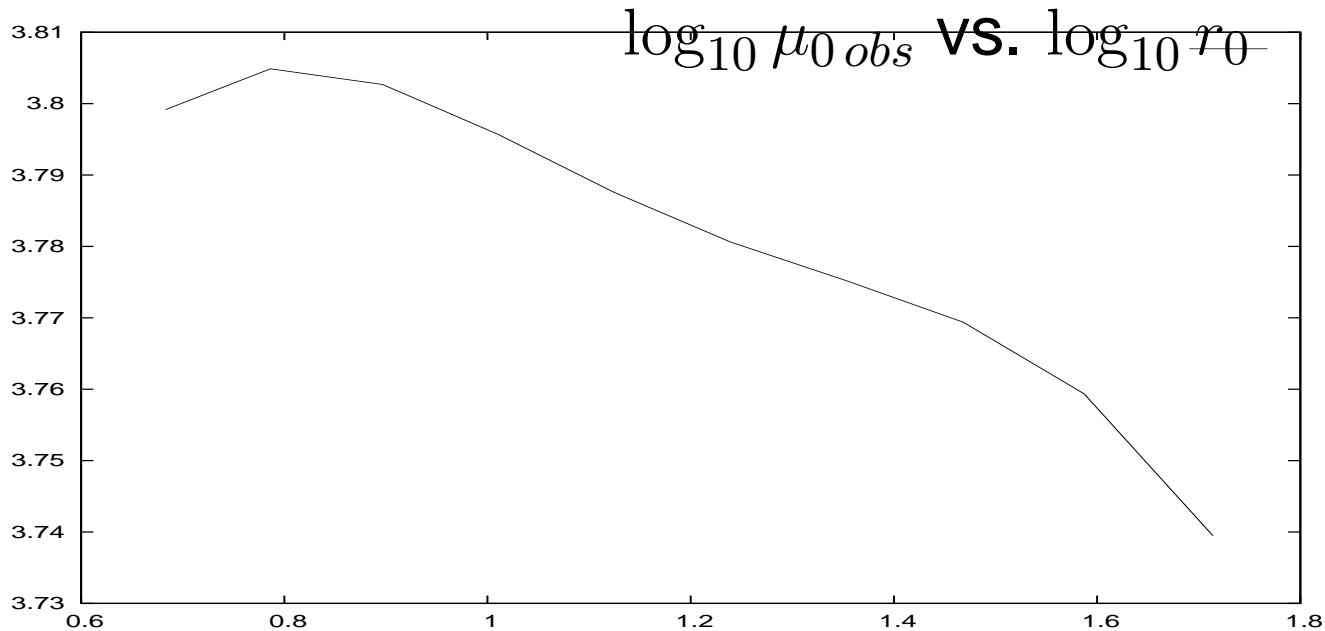


$$Q_{today} = \frac{1}{Z} Q_{prim} \quad , \quad Q \equiv \frac{\rho}{\sigma^3}$$

$\log_{10} Z$ in **solid red line** and the common logarithm of the observed phase-space density $\log_{10} Q_{halo} / (keV^4)$ in **broken green line** vs. $M_{virial} / [10^{11} M_{solar}]$.

The value of Z **depends** on the type of galaxy.
 Z is larger for spirals than for dSphs.

The observed surface density



$\log_{10} \mu_{0\text{ obs}}$ in $(\text{MeV})^3$ vs. the common logarithm of the core radius $\log_{10} r_0$ in kpc from spiral galaxies.

Both r_0 and ρ_0 vary by a factor thousand while μ_0 varies only by about $\pm 10\%$.

Relics decoupling non-relativistic

$$F_d^{NR}(p_c) = \frac{2^{\frac{5}{2}} \pi^{\frac{7}{2}}}{45} g_d Y_\infty \left(\frac{T_d}{m}\right)^{\frac{3}{2}} e^{-\frac{p_c^2}{2mT_d}} = \frac{2^{\frac{5}{2}} \pi^{\frac{7}{2}}}{45} \frac{g_d Y_\infty}{x^{\frac{3}{2}}} e^{-\frac{y^2}{2x}}$$

$Y(t) = n(t)/s(t)$, $n(t)$ number of DM particles per unit volume, $s(t)$ entropy per unit volume, $x \equiv m/T_d$, $T_d < m$.

$$Y_\infty = \frac{1}{\pi} \sqrt{\frac{45}{8}} \frac{1}{\sqrt{g_d} T_d \sigma_0 M_{Pl}} \text{ late time limit of Boltzmann.}$$

σ_0 : thermally averaged total annihilation cross-section times the velocity.

From our previous **general equations** for m and g_d :

$$m = \frac{45}{4 \pi^2} \frac{\Omega_{DM} \rho_c}{g T_\gamma^3 Y_\infty} = \frac{0.748}{g Y_\infty} \text{ eV} \quad \text{and} \quad m^{\frac{5}{2}} T_d^{\frac{3}{2}} = \frac{45}{2 \pi^2} \frac{1}{g g_d Y_\infty} Z \frac{\rho_s}{\sigma_s^{\frac{3}{2}}}$$

$$\text{Finally:} \quad \sqrt{m T_d} = 1.47 \left(\frac{Z}{g_d}\right)^{\frac{1}{3}} \text{ keV}$$

We used ρ_{DM} today **and** the decrease of the phase space density by a factor Z .

Relics decoupling non-relativistic 2

Allowed ranges for m and T_d .

$m > T_d > b$ eV where $b > 1$ or $b \gg 1$ for DM decoupling in the RD era

$$\left(\frac{Z}{g_d}\right)^{\frac{1}{3}} 1.47 \text{ keV} < m < \frac{2.16}{b} \text{ MeV} \left(\frac{Z}{g_d}\right)^{\frac{2}{3}}$$

$g_d \simeq 3$ for $1 \text{ eV} < T_d < 100 \text{ keV}$ and $1 < Z < 10^3$

$$1.02 \text{ keV} < m < \frac{104}{b} \text{ MeV} \quad , \quad T_d < 10.2 \text{ keV}.$$

Only using ρ_{DM} today (**ignoring** the phase space density information) gives **one** equation with **three** unknowns:

m , T_d and σ_0 ,

$$\sigma_0 = 0.16 \text{ pbarn} \frac{g}{\sqrt{g_d}} \frac{m}{T_d} \quad \text{http://pdg.lbl.gov}$$

WIMPS with $m = 100 \text{ GeV}$ and $T_d = 5 \text{ GeV}$ require $Z \sim 10^{23}$.

Linear results for μ_{0D} and the profile vs. observations

Since the surface density $r_0 \rho(0)$ should be **universal**, we can **identify** $r_{lin} \rho_{lin}(0)$ from a spherically symmetric solution of the **linearized** Boltzmann-Vlasov equation.

The comparison of our theoretical values for μ_{0D} and the observational value indicates that $Z \sim 10 - 1000$. Recalling the DM particle mass:

$$m = 0.568 \left(\frac{Z}{g} \right)^{\frac{1}{4}} \text{ keV for Fermions.}$$

This implies that the DM particle mass is in the **keV range**.

Remarks:

1) For larger scales nonlinear effects from small k should give the customary r^{-3} tail in the density profile.

2) The linear approximation describe the limit of **very large galaxies** with typical inner size $r_{lin} \sim 100$ kpc.

Quantum Fluctuations During Inflation and after

The Universe is homogeneous and isotropic after inflation thanks to the fast and **gigantic** expansion stretching lengths by a factor $e^{62} \simeq 10^{27}$. By the end of inflation: $T \sim 10^{14}$ GeV.

Quantum fluctuations around the classical inflaton and FRW geometry were of course **present**.

These inflationary quantum fluctuations are the **seeds** of the structure formation and of the CMB anisotropies today: galaxies, clusters, stars, planets, ...

That is, our present universe **was built** out of inflationary quantum fluctuations. CMB anisotropies spectrum:

$$3 \times 10^{-32} \text{cm} < \lambda_{\text{begin inflation}} < 3 \times 10^{-28} \text{cm}$$

$$M_{\text{Planck}} \gtrsim 10^{18} \text{ GeV} > \lambda_{\text{begin inflation}}^{-1} > 10^{14} \text{ GeV.}$$

total redshift since inflation begins till today = 10^{56} :

$$0.1 \text{ Mpc} < \lambda_{\text{today}} < 1 \text{ Gpc}, \quad 1 \text{ pc} = 3 \times 10^{18} \text{ cm} = 200000 \text{ AU}$$

Universe expansion classicalizes the physics: **decoherence**